

Title	Effect of Composition and Microstructure of Pd-Cu-Si Metallic Glassy Alloy Thin Films on Hydrogen Absorbing Properties
Author(s)	Kajita, Susumu; Kohara, Shinji; Onodera, Yohei; Fukunaga, Toshiharu; Matsubara, Eiichiro
Citation	Materials transactions (2011), 52(9): 1807-1813
Issue Date	2011-07
URL	<a href="http://hdl.handle.net/2433/171905">http://hdl.handle.net/2433/171905</a>
Right	© 2011 The Japan Institute of Metals
Type	Journal Article
Textversion	publisher

# Effect of Composition and Microstructure of Pd-Cu-Si Metallic Glassy Alloy Thin Films on Hydrogen Absorbing Properties

Susumu Kajita<sup>1</sup>, Shinji Kohara<sup>2</sup>, Yohei Onodera<sup>3</sup>, Toshiharu Fukunaga<sup>3</sup> and Eiichiro Matsubara<sup>4</sup>

<sup>1</sup>Advanced Materials Development Department, Panasonic Electric Works Co., Ltd., Kadoma 571-8686, Japan

<sup>2</sup>Research and Utilization Division, Japan Synchrotron Radiation Research Institute, Sayo-cho, Hyogo 679-5198, Japan

<sup>3</sup>Research Reactor Institute, Kyoto University, Kumatori-cho, Sennan-gun, Osaka 590-0494, Japan

<sup>4</sup>Department of Materials Science and Engineering, Kyoto University, Kyoto 606-8501, Japan

Thin films of Pd-Cu-Si metallic glassy alloys for a hydrogen sensor were fabricated by a sputtering method. In order to find out the effect of the composition and the microstructure of them on the hydrogen absorbing property (the H<sub>2</sub> response), the structural parameters based on the short-range order (SRO) were measured. Additionally, the change of the structural parameters with hydrogen absorption was measured, and the correlations of the change with the H<sub>2</sub> response and the hydrogen induced linear expansion coefficient (LEC) were examined. The H<sub>2</sub> response decreased with increases in Si content and the structural parameters. These results can be explained by the positive effects of Si content and the structural parameters on the formation of a trigonal prism which is a structural unit of Pd-based amorphous alloys, and by the negative effect of the trigonal prism on absorbing hydrogen. From the observation of the elongation of the Pd-Pd atomic distance with absorbing hydrogen, H atoms are supposed to occupy the space between Pd atoms. The amount of the change in the Pd-Pd atomic distance showed the positive correlations with the H<sub>2</sub> response and the LEC. [doi:10.2320/matertrans.M2011105]

(Received April 7, 2011; Accepted June 14, 2011; Published July 27, 2011)

**Keywords:** palladium-copper-silicon alloy, metallic glassy alloy, sputtering, thin film, hydrogen absorption, X-ray diffraction, structural analysis

## 1. Introduction

In order to develop the hydrogen sensor for fuel cell vehicles,<sup>1)</sup> we have adopted a Pd-Cu-Si metallic glassy alloy<sup>2)</sup> that is a typical composition of Pd-based metallic glassy alloys for the sensor material, and have reported its excellent hydrogen sensing ability.<sup>3,4)</sup> The hydrogen atoms dissociated from hydrogen molecules on the surface of Pd become hydrogen anions by trapping the conduction band electrons of Pd, resulting in an increase in the electric resistance of Pd.<sup>5)</sup> The high rate of change in electric resistance (that is defined as the H<sub>2</sub> response) with hydrogen absorption/desorption is required for the sensor material. The H<sub>2</sub> response increases with an increase in the amount of absorbed hydrogen in Pd and Pd-based alloys.<sup>6)</sup> Therefore, it is very important to find out the effect of the composition and the microstructure of Pd-Cu-Si metallic glassy alloys on the hydrogen absorbing property.

Several studies on hydrogen absorbing properties of Pd-based amorphous alloys have been reported. Kirchheim *et al.*<sup>7)</sup> have measured the solubility and diffusivity of hydrogen in amorphous Pd<sub>77.5</sub>Cu<sub>6</sub>Si<sub>16.5</sub> using an electrochemical method. They considered an amorphous metal was composed of a spectrum of defects, and sites which were occupied by hydrogen corresponded to different energy levels. Also they assumed the energy distribution was given by a Gaussian function and the sites were filled according to Fermi-Dirac statistics. Lee *et al.*<sup>8)</sup> have measured the solubility and diffusivity of hydrogen in amorphous Pd<sub>83</sub>Si<sub>17</sub> and Pd<sub>81</sub>Si<sub>19</sub> using an electrochemical double cell technique. They reported that the hydrogen solubility increased with increasing Pd content and decreasing Si content. Furthermore, they considered the amorphous alloy had a broad range of energy states for the hydrogen incorporation. Because there was a very strong dependence of the diffusion

coefficient on hydrogen concentration in amorphous alloys, while there was negligible dependence of it in crystallized Pd-Si alloys.

The structural analysis on Pd-based amorphous alloys has been studied using some diffraction methods. Fukunaga *et al.*<sup>9)</sup> have studied the structure of three kinds of amorphous alloys (Pd<sub>85</sub>Si<sub>15</sub>, Pd<sub>80</sub>Si<sub>20</sub> and Pd<sub>78</sub>Si<sub>22</sub>) by neutron diffraction. Ohkubo *et al.*<sup>10)</sup> have studied the structure of Pd<sub>82</sub>Si<sub>18</sub> and Pd<sub>75</sub>Si<sub>25</sub> by electron diffraction employing high-resolution electron microscopy (HREM) images. In both studies, they determined the structural parameters based on the short-range order (SRO): atomic distances of Pd-Si and Pd-Pd, the coordination number of Si atoms around a Pd atom ( $N_{\text{PdSi}}$ ) and that of Pd atoms around a Si atom ( $N_{\text{SiPd}}$ ). They discussed their obtained results with a trigonal prism which is reported as a structural unit of Pd-based amorphous alloys. In our previous report,<sup>11)</sup> we measured the structural parameters based on the SRO and explained the observed positive correlation between glass transition temperature ( $T_g$ ), which was the characteristic thermal property of metallic glassy alloys, and the composition by using the parameters on the standpoint of the formation of trigonal prisms.

The aim of this study is to find out the effect of composition and microstructure of Pd-Cu-Si metallic glassy alloy thin films on the hydrogen absorbing property (the H<sub>2</sub> response). For determining the microstructure, the structural analysis using synchrotron X-ray diffraction measurement was performed. The correlations of the H<sub>2</sub> response with the composition and the structural parameters were examined and discussed on the stand point of the formation of trigonal prisms. Additionally, the change of structural parameters with hydrogen absorption was measured, and the correlations of the change with the H<sub>2</sub> response and the hydrogen induced linear expansion coefficient (LEC) were examined.

## 2. Experimental

### 2.1 Alloy film preparation and characterization

Pd-Cu-Si alloy thin films with five kinds of composition were deposited on glass substrates using an RF magnetron sputtering equipment (L-332FHS, Cannon ANELVA Corporation) with a simultaneous three sources (Pd, Cu and Si) sputtering mechanism and a substrates-rotating mechanism. The diameters of sputtering targets (Pd, Cu and Si) were 76.2 mm each. The rotation speed of substrates was fixed at 80 rpm. The substrate-target distance (S-T distance) was 70 mm. Ar-pressure for the sputtering was 0.3 Pa. The composition ratios of thin films were controlled by changing RF powers to the three kinds of sputtering targets individually. In order to fabricate Pd-Cu-Si alloys in amorphous phase, the three constituent elements should be mixed homogeneously in a thin film. If a deposition rate (deposition thickness per one revolution of substrates) of an element is larger than its atomic diameter, it leads to the formation of a single element layer in principle. For obtaining the structure of homogeneously mixed elements, a sparse deposition per one revolution of substrates is required. Therefore, the RF power was controlled so that the deposition rate of each element became smaller than the corresponding atomic diameter.

The deposition time was calculated to achieve 4000 nm thickness of Pd-Cu-Si thin films using the total deposition rate which is the sum of the deposition rates of three kinds of elements. After measuring the thickness of a deposited thin film, the total deposition rate was corrected according to the difference between the measured thickness and 4000 nm. After that, a 100 nm thickness of Pd-Cu-Si thin film was fabricated by using the corrected total deposition rate. The thicknesses of thin films were measured with a surface profiler (Dektak<sup>3</sup> ST, Veeco Instruments Inc.). The thin films of 100 nm thickness were used for the measurement of the H<sub>2</sub> response and those of 4000 nm thickness were used for the X-ray diffraction measurement and the characterization of the films. The composition of the thin films was analyzed by inductively coupled plasma-atomic emission spectrometry (ICP-AES).

### 2.2 Measurement of the H<sub>2</sub> response

The H<sub>2</sub> response was observed by measuring the electric resistance change of the thin films exposed in N<sub>2</sub> and H<sub>2</sub> under the atmospheric pressure. A thin film sample with a glass substrate was placed in a stainless chamber set up in an electric oven and then its electric resistance was measured by 4-probe method using Au plated brass electrodes, while the thin film sample was exposed in 100% N<sub>2</sub> and 100% H<sub>2</sub> of atmospheric pressure alternately. The experimental temperature was controlled at 303 K. The H<sub>2</sub> response is expressed as the normalized value ( $R/R_0$ ), where  $R$  and  $R_0$  are the electric resistances of the thin film exposed in 100% H<sub>2</sub> and 100% N<sub>2</sub>, respectively. The detail of the H<sub>2</sub> response measurement was explained in the previous reports.<sup>3,4)</sup>

### 2.3 Measurement of the hydrogen induced linear expansion coefficient

The hydrogen induced linear expansion coefficients

(LECs) of thin films were measured with a thermo mechanical analyzer (TMA, TMA4030SA, Bruker AXS K.K.) by tensile loading method. The sample for the measurement was a 4000 nm thickness, 10 mm length and 5 mm width thin film which was peeled off from a glass substrate and was cut into the size. The load in tension was 0.5 g. Operating temperature was 298 K. First, the sample was exposed in 100% N<sub>2</sub>. After that, the atmosphere gas was changed to 100% H<sub>2</sub> and the longitudinal expansion of the sample was measured. The hydrogen induced LEC was calculated by the following equation.

$$\text{LEC (\%)} = (L_{\text{H}_2} - L_0)/L_0 \times 100$$

$L_{\text{H}_2}$ : length of the sample exposed in 100% H<sub>2</sub>

$L_0$ : initial length of the sample (= 10 mm)

The longitudinal expansion of the sample is expressed as ( $L_{\text{H}_2} - L_0$ ).

### 2.4 X-ray diffraction measurement

In order to determine the structural parameters on the SRO, synchrotron X-ray diffraction measurement of thin films in hydrogen desorbing/absorbing condition was performed. The prepared thin films of about 4000 nm thickness were peeled off from glass substrates, and were cut into 9 mm square films. 40 pieces of the cut thin films were stacked in a stainless sample holder having two windows covered with 0.125 mm thickness polyimide films and a stop valve. The atmosphere in the sample holder was air of atmospheric pressure for hydrogen desorbing condition. When the measurement was carried out in hydrogen absorbing condition, the air in the stainless sample holder was substituted with 100% H<sub>2</sub> of atmospheric pressure with a dry pump.

The synchrotron X-ray diffraction measurements were carried out using a horizontal two-axis diffractometer with a photon energy of 61.57 keV ( $\lambda = 0.02014$  nm) at the BL04B2 beamline of the SPring-8 synchrotron radiation facility. The temperature during the measurement was about 293 K. After corrections for background, polarization, absorption and Compton scattering, the scattering intensity was normalized to give the structure factor,  $S(Q)$ , where  $Q = 4\pi \sin \theta/\lambda$ .<sup>12)</sup>

## 3. Results and Discussion

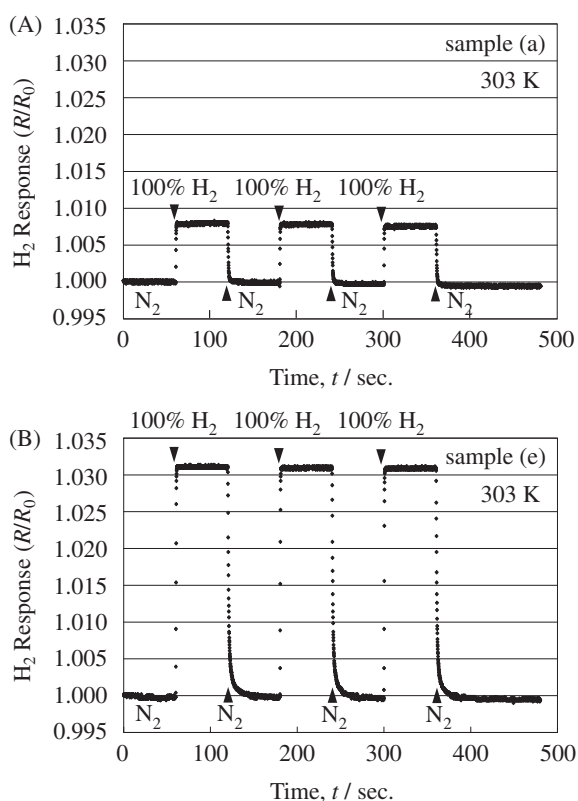
### 3.1 H<sub>2</sub> response

Table 1 shows the composition and the H<sub>2</sub> response of the thin films, samples (a) to (e), measured at 303 K. Figures 1(A) and (B) show the 100% H<sub>2</sub> response transients of sample (a) Pd<sub>67.8</sub>Cu<sub>14.3</sub>Si<sub>17.9</sub> and sample (e) Pd<sub>75.1</sub>Cu<sub>12.3</sub>-Si<sub>12.6</sub> at 303 K, respectively. These figures indicate significant difference in the 100% H<sub>2</sub> response depending on the composition.

In order to examine the correlation between the composition and the H<sub>2</sub> response, the H<sub>2</sub> responses against Pd content and Si content are plotted in Figs. 2(A) and (B), respectively. The described codes (a) to (e) are corresponding to the samples shown in Table 1. The H<sub>2</sub> response increases with increasing Pd content in Fig. 2(A). This result can be explained clearly by that Pd is a primary element which absorbs hydrogen in a Pd-Cu-Si alloy, and by that the electric

Table 1 Composition and H<sub>2</sub> response ( $R/R_0$ ) at 303 K of fabricated thin films.

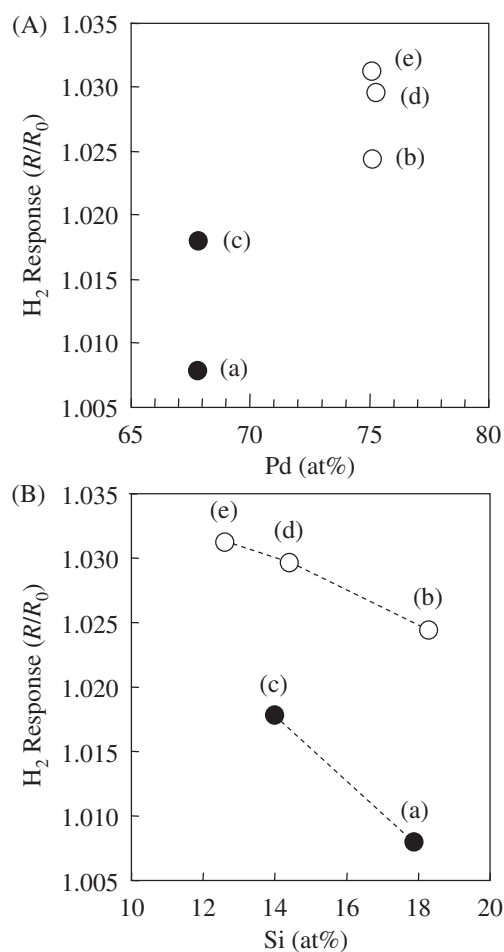
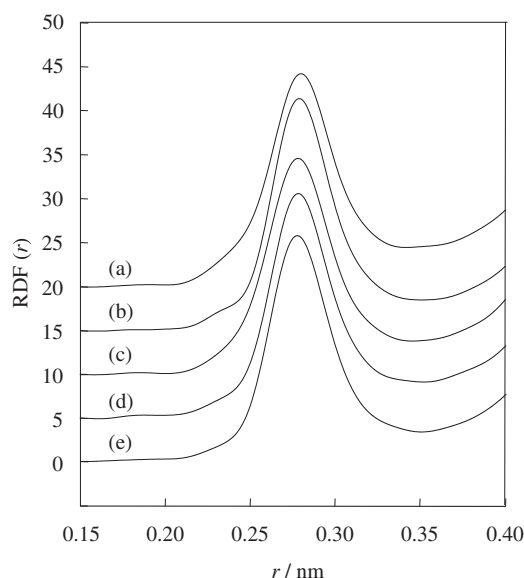
Sample	composition	H <sub>2</sub> Response ( $R/R_0$ ) at 303 K
(a)	Pd <sub>67.8</sub> Cu <sub>14.3</sub> Si <sub>17.9</sub>	1.0079
(b)	Pd <sub>75.1</sub> Cu <sub>6.6</sub> Si <sub>18.3</sub>	1.0244
(c)	Pd <sub>67.7</sub> Cu <sub>18.2</sub> Si <sub>14.1</sub>	1.0178
(d)	Pd <sub>75.3</sub> Cu <sub>10.3</sub> Si <sub>14.4</sub>	1.0296
(e)	Pd <sub>75.1</sub> Cu <sub>12.3</sub> Si <sub>12.6</sub>	1.0312

Fig. 1 100% H<sub>2</sub> response transients of Pd-Cu-Si metallic glassy alloy thin films at 303 K. (A) sample (a) Pd<sub>67.8</sub>Cu<sub>14.3</sub>Si<sub>17.9</sub> and (B) sample (e) Pd<sub>75.1</sub>Cu<sub>12.3</sub>Si<sub>12.6</sub>.  $R$ : electric resistance of the sample in 100% H<sub>2</sub>,  $R_0$ : electric resistance of the sample in 100% N<sub>2</sub>. Gas-changing interval was 60 s.

resistance of the alloy changes depending on the amount of absorbed hydrogen. In Fig. 2(B), the data are classified into two groups according to their Pd content (Pd = 75.1–75.3 at% and Pd = 67.8 at%) to eliminate the strong effect of Pd content on the H<sub>2</sub> response. From Fig. 2(B), it can be seen that H<sub>2</sub> response decreases with increasing Si content in the same group. This suggests the possibility of some kind of correlation between the structural changes in the thin films with increasing Si content and the H<sub>2</sub> response relating to the amount of absorbed hydrogen.

### 3.2 Structural analysis

The structural parameters based on the SRO of the thin films were measured. Basically, the structural parameters in hydrogen desorbing condition and the analyzing procedure in the present study are the same as those in the previous report.<sup>11)</sup> Figure 3 shows the first peaks of radial distribution

Fig. 2 100% H<sub>2</sub> response at 303 K as functions of (A) Pd content and (B) Si content. ○ Pd = 75.1–75.3 at% ● Pd = 67.8 at%Fig. 3 First peaks of radial distribution functions,  $RDF(r)$ s, of samples (a) to (e) measured in hydrogen desorbing condition.

functions,  $RDF(r)$ s, of samples (a) to (e). The method for obtaining the  $RDF(r)$  is explained in a reference.<sup>13)</sup>

In order to obtain the structural parameters, it is necessary to divide the first peak of  $RDF(r)$  into partial correlations by

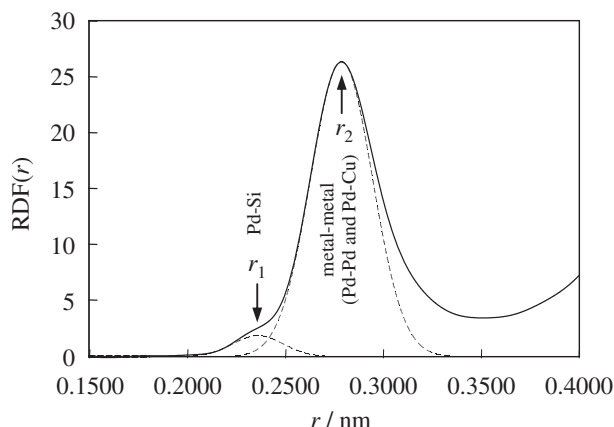


Fig. 4 The first peak of radial distribution function,  $RDF(r)$ , of sample (b) measured in hydrogen desorbing condition. Broken lines indicate the Gaussian peaks corresponding to the Pd-Si and metal-metal (Pd-Pd and Pd-Cu) pair correlations positioned at  $r_1$  and  $r_2$ , respectively.

the least square fitting with Gaussian functions. As an example of it, Fig. 4 shows the first peak of  $RDF(r)$  of sample (b) with two Gaussian peaks (positioned at  $r_1$  and  $r_2$ ) indicating by broken lines. The two Gaussian peaks ( $r_1$  and  $r_2$ ) are corresponding to Pd-Si and metal-metal (Pd-Pd and Pd-Cu) pair correlations, respectively. Pd-Cu-Si metallic glassy alloys have 6 kinds of pair correlations: Pd-Pd, Pd-Cu, Pd-Si, Cu-Cu, Cu-Si and Si-Si. However, we ignored the pair correlations of Cu-Cu, Cu-Si and Si-Si for the Gaussian peak-fitting, because their calculated weighting factors were negligibly small compared to those of the other pair correlations. The weighting factor ( $W_{ij}$ ) for the pair correlation between an  $i$ -atom and a  $j$ -atom is defined as follows:<sup>13)</sup>

$$W_{ij} = \frac{c_i c_j f_i f_j}{\langle f \rangle^2}$$

$$\langle f \rangle^2 = \left( \sum_i c_i f_i \right)^2$$

where  $c_i$  and  $f_i$  are the concentration and atomic scattering factor of the component atoms  $i$ , respectively. For example, the weighting factors of sample (b)  $Pd_{75.1}Cu_{6.6}Si_{18.3}$  are calculated as follows:  $W_{PdPd} = 0.784$ ,  $2W_{PdCu} = 0.087$ ,  $2W_{PdSi} = 0.116$ ,  $W_{CuCu} = 0.002$ ,  $2W_{CuSi} = 0.006$  and  $W_{SiSi} = 0.004$ .

For dividing the first peak of  $RDF(r)$  into the Gaussian peaks corresponding to Pd-Pd, Pd-Cu and Pd-Si pair correlations, the positions of them should be fixed at first. The peak positions corresponding to pair correlations are defined as the atomic distances of the pair atoms. As for the atomic distances of Pd-Si and Pd-Pd, we used previous studies on the structure of Pd-Si amorphous alloys as a reference. The structural parameters reported by Fukunaga *et al.*<sup>9)</sup> and Ohkubo *et al.*<sup>10)</sup> are summarized in Table 2. The atomic distances of Pd-Si and Pd-Pd are 0.242–0.248 nm and 0.275–0.281 nm, respectively.  $N_{ij}$  in Table 2 expresses the coordination number of  $j$ -atoms around an  $i$ -atom.

The atomic distance of Pd-Cu can be roughly estimated by calculating the sum of atomic radiuses of Pd atom and Cu atom. The atomic radiuses of Pd atom and Cu atom are

Table 2 Structural parameters of Pd-Si amorphous alloys reported in previous studies.<sup>9,10)</sup>

measurement	neutron diffraction <sup>9)</sup>			electron diffraction <sup>10)</sup>	
Glass sample	$Pd_{85}Si_{15}$	$Pd_{80}Si_{20}$	$Pd_{78}Si_{22}$	$Pd_{82}Si_{18}$	$Pd_{75}Si_{25}$
Pd-Si atomic distance/nm	0.242	0.242	0.243	0.242	0.248
$N_{SiPd}$	7.3	6.6	6.3	9.1	8.8
$N_{PdSi}$	1.2	1.6	1.8	2.0	2.9
Pd-Pd atomic distance/nm	0.278	0.280	0.281	0.275	0.279
$N_{PdPd}$	10.5	10.6	10.1	12.1	11.0

0.137 nm and 0.128 nm, respectively, thereby the atomic distance of Pd-Cu should be about 0.265 nm. Therefore, the Gaussian peak corresponding to Pd-Cu pair correlation should mainly belong to the  $r_2$ -positioned peak in Fig. 4. However, we could not divide the  $r_2$ -positioned peak into two Gaussian peaks corresponding to Pd-Pd and Pd-Cu pair correlations. The atomic distance of Pd-Pd is about 0.28 nm from the previous studies summarized in Table 2. The atomic distances of Pd-Pd and Pd-Cu are very close and additionally,  $W_{PdPd}$  is much larger than  $W_{PdCu}$ . Therefore, the Gaussian peak of Pd-Cu will be so small that it will certainly be buried in the large peak of Pd-Pd completely. From this reason, we treated  $r_2$  as the Pd-Pd atomic distance, although the  $r_2$ -positioned peak was corresponding to metal-metal (Pd-Pd and Pd-Cu) pair correlations. The peak position ( $r_1$ ) was defined as the atomic distance of Pd-Si.

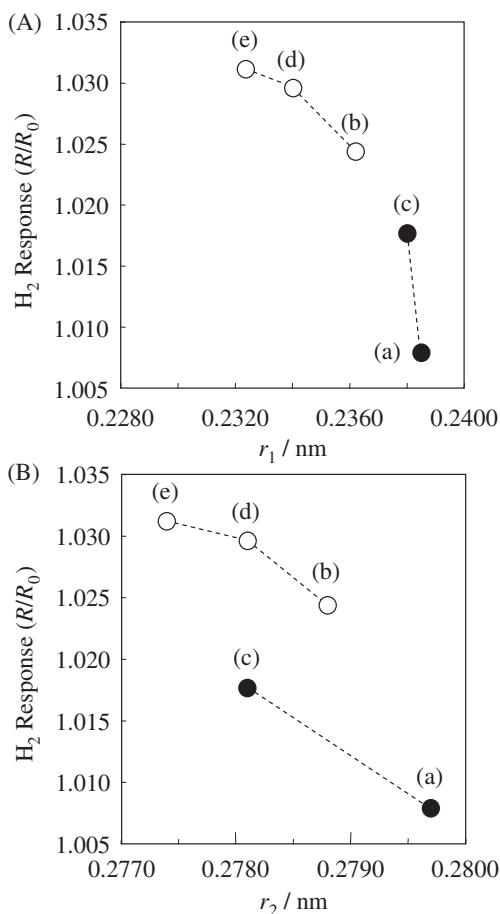
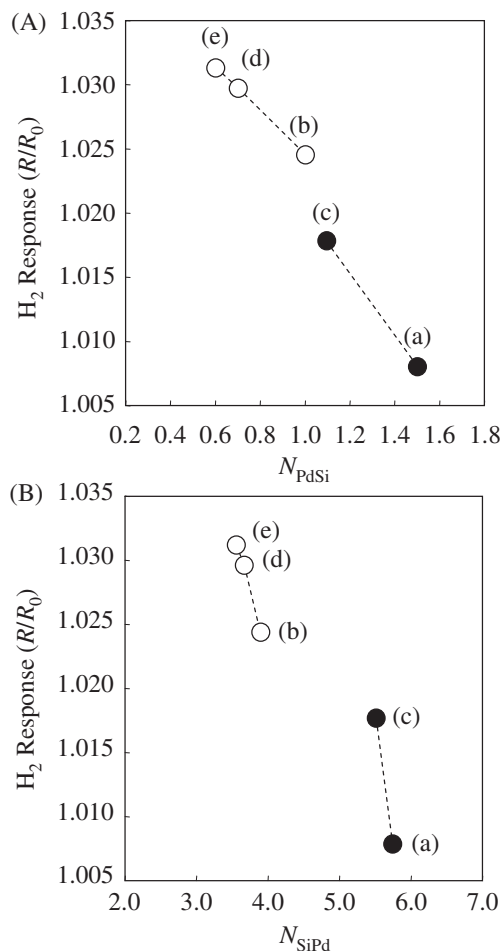
For dividing the first peak of  $RDF(r)$  into two Gaussian peaks, the peak position appearing at around 0.28 nm was assigned as  $r_2$  at first and then, the Gaussian peak-fitting of  $r_2$  was performed. After that, the Gaussian peak positioned at  $r_1$  was fitted at around 0.24 nm. The coordination numbers ( $N_{PdSi}$  and  $N_{SiPd}$ ) were calculated using the area of the Gaussian peak positioned at  $r_1$ , weighting factors ( $W_{PdSi}$  and  $W_{SiPd}$ ) and the contents (Si content and Pd content). The calculation method of them is explained in a reference.<sup>14)</sup> The structural parameters ( $r_1$ ,  $r_2$ ,  $N_{PdSi}$  and  $N_{SiPd}$ ) of samples (a) to (e) in hydrogen desorbing/absorbing condition were obtained by this procedure. They are summarized in Table 3. As we mentioned above, the peak positions ( $r_1$  and  $r_2$ ) are corresponding to the atomic distances (Pd-Si and Pd-Pd), respectively. Comparing the structural parameters in hydrogen desorbing/absorbing conditions, we can see the peak position ( $r_1$ ),  $N_{PdSi}$  and  $N_{SiPd}$  are about the same values. In contrast, a small change can be seen between their peak positions ( $r_2$ ).

### 3.3 Effect of the structural parameters on the H<sub>2</sub> response

The H<sub>2</sub> responses against  $r_1$  and  $r_2$  measured in hydrogen desorbing condition are plotted in Figs. 5(A) and (B), respectively. The described codes (a) to (e) are corresponding to the samples shown in Table 1. The data are classified into two sample groups according to Pd content (Pd = 75.1–75.3 at% and 67.8 at%) to eliminate the strong effect of Pd content on the H<sub>2</sub> response. By comparing the data in the same Pd content groups, it can be seen that the H<sub>2</sub> responses

Table 3 Coordination number ( $N_{ij}$ ) and peak positions ( $r_1$  and  $r_2$ ) of samples (a) to (e) calculated from RDF( $r$ )s measured in hydrogen desorbing/absorbing condition.

Sample	composition	in hydrogen desorbing condition				in hydrogen absorbing condition			
		$r_1/\text{nm}$	$N_{\text{PdSi}}$	$N_{\text{SiPd}}$	$r_2/\text{nm}$	$r_1/\text{nm}$	$N_{\text{PdSi}}$	$N_{\text{SiPd}}$	$r_2/\text{nm}$
(a)	Pd <sub>67.8</sub> Cu <sub>14.3</sub> Si <sub>17.9</sub>	0.2385	1.5	5.7	0.2797	0.2385	1.5	5.8	0.2797
(b)	Pd <sub>75.1</sub> Cu <sub>6.6</sub> Si <sub>18.3</sub>	0.2362	1.0	3.9	0.2788	0.2362	1.0	3.9	0.2791
(c)	Pd <sub>67.7</sub> Cu <sub>18.2</sub> Si <sub>14.1</sub>	0.2380	1.1	5.5	0.2781	0.2380	1.1	5.4	0.2781
(d)	Pd <sub>75.3</sub> Cu <sub>10.3</sub> Si <sub>14.4</sub>	0.2340	0.7	3.7	0.2781	0.2340	0.7	3.7	0.2784
(e)	Pd <sub>75.1</sub> Cu <sub>12.3</sub> Si <sub>12.6</sub>	0.2324	0.6	3.6	0.2774	0.2324	0.6	3.6	0.2780

Fig. 5 100% H<sub>2</sub> response at 303 K as functions of peak positions, (A)  $r_1$  and (B)  $r_2$ , of RDF( $r$ )s measured in hydrogen desorbing condition. ○ Pd = 75.1–75.3 at% ● Pd = 67.8 at%Fig. 6 100% H<sub>2</sub> response at 303 K as functions of coordination numbers, (A)  $N_{\text{PdSi}}$  and (B)  $N_{\text{SiPd}}$ , in hydrogen desorbing condition. ○ Pd = 75.1–75.3 at% ● Pd = 67.8 at%

decrease with increases in  $r_1$  and  $r_2$ . The H<sub>2</sub> responses against  $N_{\text{PdSi}}$  and  $N_{\text{SiPd}}$  measured in hydrogen desorbing condition are plotted in Figs. 6(A) and (B), respectively, with data classification by Pd content. The H<sub>2</sub> responses decrease with increases in  $N_{\text{PdSi}}$  and  $N_{\text{SiPd}}$  in the same Pd content groups.

Concerning the effect of the structural parameters on the microstructure of Pd-based amorphous alloys, Fukunaga *et al.*<sup>9)</sup> have reported their study as follows. They supposed that with increasing Si content, the three-dimensional arrangement of neighboring Pd atoms around a Si atom was likely to become more trigonal prismatic coordination in Pd-Si amorphous alloys. And also, their obtained structural parameters, the atomic distances (Pd-Si and Pd-Pd) and  $N_{\text{PdSi}}$ , increase with increasing Si content. Consequently, it can be

stated that increases in the structural parameters with Si content suggests an increase in the number density of trigonal prisms. The obtained results in Figs. 2, 5 and 6 were considered on the basis of this theory by Fukunaga *et al.* In Fig. 2(B), the H<sub>2</sub> response decreases with increasing Si content. Considering the positive correlation between Si content and the number density of trigonal prisms, it can be stated that the H<sub>2</sub> response has negative correlation with the number density of trigonal prisms. In Figs. 5(A) and (B) and Fig. 6(A), the H<sub>2</sub> responses decrease with increases in the structural parameters ( $r_1$ ,  $r_2$  and  $N_{\text{PdSi}}$ ). Because the structural parameters have positive correlation with the number density of trigonal prisms, it also can be stated that the H<sub>2</sub> response

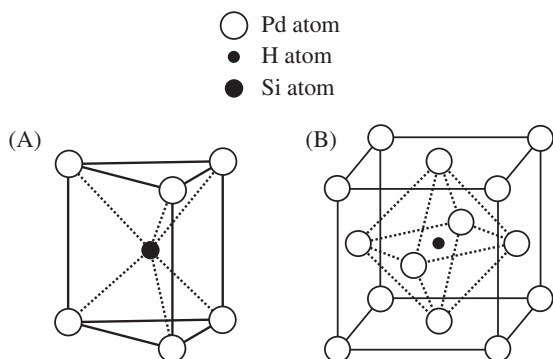


Fig. 7 Schematic illustrations of (A) trigonal prism<sup>9)</sup> (6 Pd atoms around a Si atom) and (B) a H atom in octahedral interstitial site in fcc-Pd.

has negative correlation with the number density of trigonal prisms. Additionally, this negative correlation can be seen in Fig. 6(B). Samples (a) and (c) which showed lower H<sub>2</sub> response in all samples indicated  $N_{\text{SiPd}}$  (in hydrogen desorbing condition) of 5.7 and 5.5, respectively (see Table 3). These values are close to 6 of  $N_{\text{SiPd}}$  of a trigonal prism illustrated in Fig. 7(A).<sup>9)</sup> This result suggests that samples (a) and (c) have more trigonal prismatic structures than the other samples.

The negative effect of the trigonal prisms on the H<sub>2</sub> response was considered on the standpoint of the crystal lattice structure. A H atom absorbed in Pd can occupy the octahedral interstitial site in fcc-Pd as illustrated in Fig. 7(B). In contrast, a trigonal prism has 6 Pd atoms at 6 vertices and a Si atom in its central hole as illustrated in Fig. 7(A). The trigonal prism has no interstitial site where a H atom can stably occupy because a Si atom occupies the central position of the prism, while fcc-Pd has octahedral interstitial site for occupying a H atom. However, a Pd-Cu-Si metallic glassy alloy is supposed to have not only trigonal prisms but also disordered Pd atoms, Pd-clusters and Pd-nanocrystals. Pd-nanocrystals have the size of several nanometers to tens nanometers. Pd-clusters mean the clusters of several to several hundreds of Pd-atoms. Pd-clusters positively include the clusters of a Pd-crystal and a Pd-atom, and their size is far smaller than that of Pd-nanocrystals. H atoms are supposed to occupy the space between Pd atoms. Especially in the case of fcc-Pd, H atoms are supposed to occupy the octahedral interstitial site.

### 3.4 Change of structural parameters with hydrogen absorption

Figure 8 shows the shifts of the first peaks in RDF( $r$ ) induced by absorbed hydrogen at 293 K. Solid lines and broken lines express the RDF( $r$ )s of thin films measured in hydrogen desorbing (without H) and absorbing (with H) conditions, respectively. The peak positions are corresponding to  $r_2$  which indicates the Pd-Pd atomic distance. Samples (a) and (c) which indicated lower H<sub>2</sub> response show less peak shifts. On the other hand, samples (b), (d) and (e) show the clear peak shifts though the shifts are very small.

The peak shift ( $\Delta r_2$ ) is defined as ( $\Delta r_2 = r_2$  with H -  $r_2$  without H). The H<sub>2</sub> response is plotted against the peak shift in Fig. 9. From this figure, we can see the positive correlation

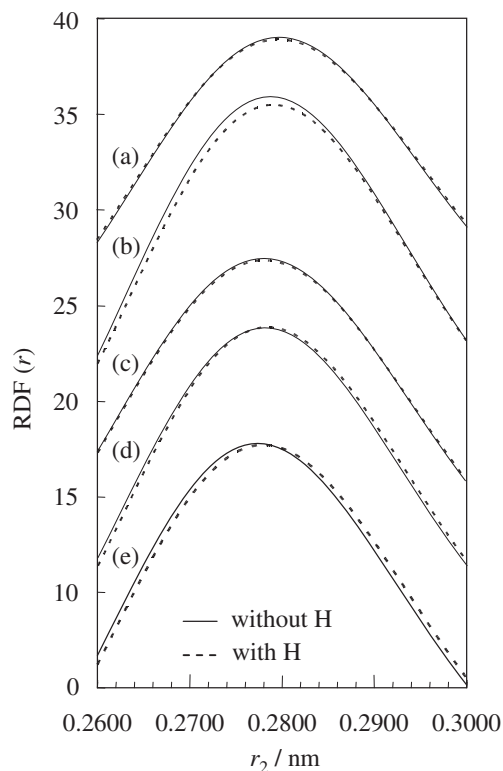


Fig. 8 Shifts of the first peaks in RDF( $r$ )s induced by absorbed hydrogen at 293 K. Solid lines indicate RDF( $r$ )s in hydrogen desorbing condition (without H). Broken lines indicate RDF( $r$ )s in hydrogen absorbing condition (with H).

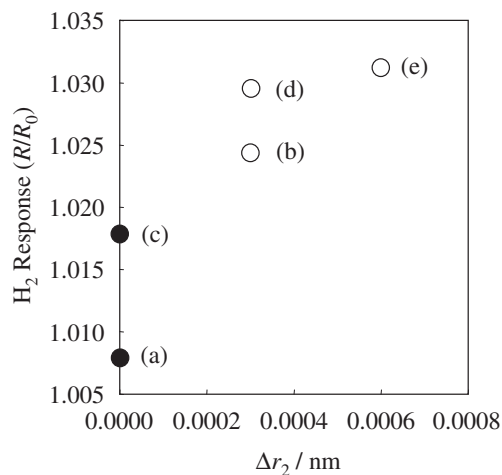


Fig. 9 100% H<sub>2</sub> response at 303 K as a function of  $\Delta r_2$ .  $\Delta r_2 = r_2$  with H -  $r_2$  without H ○ Pd = 75.1–75.3 at% ● Pd = 67.8 at%

between the H<sub>2</sub> response and  $\Delta r_2$ . As we mentioned above,  $r_2$  is defined as the Pd-Pd atomic distance. Therefore, the increase in  $r_2$  caused by hydrogen absorption can be taken as the elongation of Pd-Pd atomic distance. The Pd-Pd atomic distance is thought to be elongated by the occupation of H atoms in the space between Pd atoms. The elongation of Pd-Pd atomic distances should lead to the volume expansion of thin films. The linear expansion coefficient (LEC) measured at 298 K is plotted against  $\Delta r_2$  in Fig. 10, and it increases approximately linearly with increasing  $\Delta r_2$  as expected.

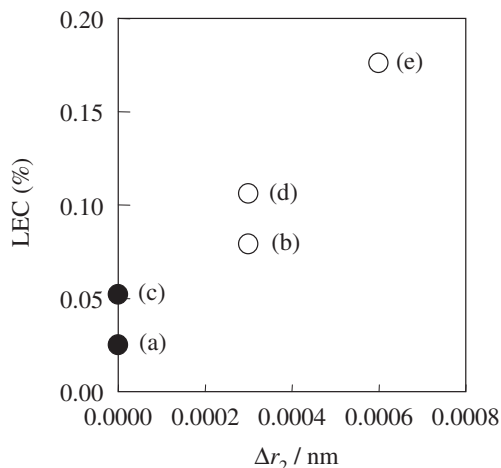


Fig. 10 100% H<sub>2</sub> induced linear expansion coefficient (LEC) at 298 K as a function of  $\Delta r_2$ .  $\Delta r_2 = r_2$  with H -  $r_2$  without H ○ Pd = 75.1–75.3 at% ● Pd = 67.8 at%

In Fig. 9, the correlation between the H<sub>2</sub> response and  $\Delta r_2$  is not linear, because of the slight low value of the H<sub>2</sub> response of sample (e), while the LEC and  $\Delta r_2$  show linear positive correlation. The reason of the low H<sub>2</sub> response of sample (e) can be explained by the mechanism which we have reported in the previous study.<sup>15)</sup> The mechanism is summarized as follows. The sample with high Pd/Si ratio (Pd/Si  $\geq$  5.96 in the previous study) has many Pd-nanocrystals in the amorphous matrix which probably includes Pd-clusters and disordered Pd atoms as well as trigonal prisms. When the sample is exposed in H<sub>2</sub>, the Pd-nanocrystals form the electric contacts with each other by the connection of volume expanded Pd-clusters induced by absorbed hydrogen, resulting in a decrease in the electric resistance. That is the conflicting behavior with an increase by hydrogenation of Pd. In this case, the H<sub>2</sub> response takes lower value than that estimated from the hydrogenation of Pd, because the H<sub>2</sub> response is derived from the sum of the electric resistances relating to the two conflicting behavior. Therefore, the sample with Pd-nanocrystals indicates the low H<sub>2</sub> response for the amount of absorbed hydrogen by it. Pd/Si ratio of sample (e) is larger than those of the other samples: Pd/Si = (a) 3.79, (b) 4.10, (c) 4.84, (d) 5.23 and (e) 5.96. On the other hand, LEC has linear positive correlation with the amount of absorbed hydrogen whether the Pd-nanocrystals exist or not. From this reason, sample (e) is supposed to indicate the low H<sub>2</sub> response for its high LEC.

#### 4. Summary

In this study, Pd-Cu-Si metallic glassy alloy thin films were fabricated by a sputtering method, and the correlations of the H<sub>2</sub> response with the composition and the structural parameters based on the short-range order (SRO) were examined. Additionally, the change of structural parameters with hydrogen absorption was measured, and the correlations of the change with the H<sub>2</sub> response and the hydrogen induced

linear expansion coefficient (LEC) were examined. The obtained results are summarized as follows.

- (1) The H<sub>2</sub> response increased with increasing Pd content and decreased with increasing Si content.
- (2) The H<sub>2</sub> response decreased with increases in the structural parameters: the atomic distances (Pd-Si and Pd-Pd) and the coordination numbers ( $N_{\text{PdSi}}$  and  $N_{\text{SiPd}}$ ). The increases in Si content and the structural parameters can be related to an increase in the number density of trigonal prisms. Therefore, it can be stated that the H<sub>2</sub> response and the amount of absorbed hydrogen have negative correlations with the number density of trigonal prisms. Possible explanation for this result is that the trigonal prism has no interstitial site where a H atom can stably occupy because of a Si atom occupying the central position of the prism.
- (3) The elongation of the Pd-Pd atomic distance with absorbing hydrogen was observed by the peak shift of RDF( $r$ ). From this result, H atoms are supposed to occupy the space between Pd atoms. The peak shift showed the positive correlations with the H<sub>2</sub> response and the hydrogen induced LEC. In other words, the Pd-Pd atomic distance increased with an increase in the amount of absorbed hydrogen to increase the volume expansion of thin films.

#### Acknowledgments

The authors would like to thank Dr. K. Ohara for his assistance in X-ray diffraction measurement. The synchrotron radiation experiments were approved by the Japan Synchrotron Radiation Research Institute (proposal numbers: 2008B1074 and 2009A1078).

#### REFERENCES

- 1) U.S. Department of Energy: Fuel Cells, Technical Plan, Multi-Year Research, Development and Demonstration Plan (2007).
- 2) H. S. Chen and D. Turnbull: *Acta Metall.* **17** (1969) 1021–1031.
- 3) S. Kajita, S. Yamaura, H. Kimura, K. Yubuta and A. Inoue: *IEE Trans. SM* **128** (2008) 225–229.
- 4) S. Kajita, S. Yamaura, H. Kimura and A. Inoue: *Sens. Actuators B* **150** (2010) 279–284.
- 5) Y. Ohsumi: *Hydrogen Storage Alloy*, (AGNE Gijyutu Center, Tokyo, 2000) p. 72.
- 6) F. A. Lewis: *The Palladium Hydrogen System*, (Academic Press, London, 1967) p. 11.
- 7) R. Kirchheim, F. Sommer and G. Schluckebier: *Acta Metall.* **30** (1982) 1059–1068.
- 8) Y. S. Lee and D. A. Stevenson: *J. Non-Cryst. Solids* **72** (1985) 249–266.
- 9) T. Fukunaga and K. Suzuki: *Sci. Rep. Insts Tohoku Univ. A* **29** (1981) 153–175.
- 10) T. Ohkubo, Y. Hirotsu and M. Matsushita: *J. Electron Microsc.* **48** (1999) 1005–1013.
- 11) S. Kajita, S. Kohara, Y. Onodera, T. Fukunaga and E. Matsubara: *Mater. Trans.* **52** (2011) 1349–1355.
- 12) S. Kohara, M. Itou, K. Suzuya, Y. Inamura, Y. Sakurai, Y. Ohishi and M. Takata: *J. Phys. Condens. Matter* **19** (2007) 506101.
- 13) T. Fukunaga: *JIM Seminar Text 73*, (THE JAPAN INSTITUTE OF METALS, Japan, 1997) p. 107.
- 14) Y. Waseda and E. Matsubara: *X-ray Structural Analysis*, (UCHIDA ROKAKUHO PUBLISHING CO., LTD., Japan, 1998) p. 213.
- 15) S. Kajita, Y. Hasebe, T. Fukunaga and E. Matsubara: *Mater. Trans.* **52** (2011) 1148–1155.